Chemosphere 288 (2022) 132506

Contents lists available at ScienceDirect

Chemosphere

journal homepage: www.elsevier.com/locate/chemosphere

Caffeine photocatalytic degradation using composites of NiO/TiO_2–F and CuO/TiO_2–F under UV irradiation

Claudia Castañeda [a,**], José J. Martínez [a], Laura Santos [a], Hugo Rojas [a], Sameh M. Osman [b], Ricardo Gómez [c], Rafael Luque [d,e,*]

[a] Universidad Pedagógica y Tecnológica de Colombia, Escuela de Ciencias Química, Grupo de Catálisis-UPTC, Avenida Central de Norte, Vía Paipa, Tunja, Boyacá, Colombia
[b] Chemistry Department, College of Science, King Saud University, P.O. Box 2455, Riyadh, 11451, Saudi Arabia
[c] Universidad Autónoma Metropolitana-Iztapalapa, Depto. De Química, México, D.F. Mexico
[d] Grupo FQM-383, Departamento de Química Orgánica, Universidad de Córdoba, Campus Universitario de Rabanales, Edificio Marie Curie (C3), E-14014, Córdoba, Spain
[e] Peoples Friendship University of Russia (RUDN University), 6 Miklukho-Maklaya str., 117198, Moscow, Russia

HIGHLIGHTS

- Caffeine, a persistent and toxic emergent compound, could be easily degraded using CuO or NiO on TiO_2–F.
- A caffeine photodegradation of 90 and 88% was reached using CuO/TiO_2–F and NiO/TiO_2–F, respectively.
- TiO_2–F coupled with CuO and NiO increase the effective separation of the charge carriers.
- CuO/TiO_2–F and NiO/TiO_2–F shown a rate of hydroxyl radical generation 2.2 and 1.5 higher than that achieved using the TiO_2–F.

GRAPHICAL ABSTRACT

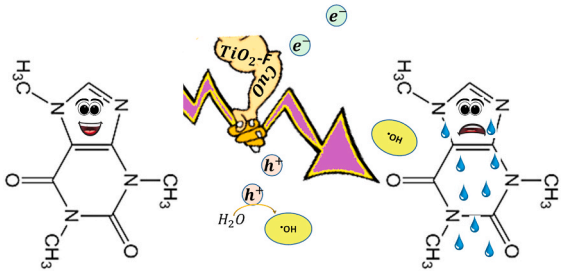

ARTICLE INFO

Handling Editor: Jun Huang

Keywords:
Caffeine
Degradation
Photocatalysis
NiO/TiO_2–F
CuO/TiO_2–F
Emerging contaminants

ABSTRACT

The interest in the removal of emerging contaminants has increased in the last decade. Photocatalytic degradation using p-n heterojunctions could effectively provide the degradation of these type of substances that are persistent in the environment. In this work, the synthesis, characterization, and photocatalytic evaluation of TiO_2–F as well as CuO/TiO_2–F and NiO/TiO_2–F composite materials were studied in the photo-assisted degradation of caffeine using UV radiation. The fluorination of titanium dioxide induced changes in some physicochemical properties of the materials, which contributed to a decrease in surface area and bandgap energy as well as an increase in crystallite size as compared to pristine TiO_2. ≡Ti–F species were evidenced to be formed, which could favor charge separation processes. A highest segregation of CuO species in comparison with NiO on the surface of TiO_2–F could be formed, which could increase defect sites and decrease the band gap. The formation of a heterojunction between the semiconductors was evidenced, responsible for the observed improvements in photocatalytic properties of the composite materials. The photocatalytic tests evidenced an important

* Corresponding author. Grupo FQM-383, Departamento de Química Orgánica, Universidad de Córdoba, Campus Universitario de Rabanales, Edificio Marie Curie (C3), E-14014 Córdoba, Spain.
** Corresponding author.
E-mail addresses: claudia.castaneda@uptc.edu.co (C. Castañeda), rafael.luque@uco.es (R. Luque).

https://doi.org/10.1016/j.chemosphere.2021.132506
Received 3 August 2021; Received in revised form 27 September 2021; Accepted 6 October 2021
Available online 14 October 2021

degradation of caffeine; however, mineralization was incomplete. The stability of the composite materials and their potential use in the photocatalytic treatment of caffeine was evaluated by reuse tests.

1. Introduction

The continuous appearance of novel chemicals in water systems is a reflection of the habits of modern life, which establishes a priority in research on wastewater treatment and sustainable development (Zhang et al., 2019; Li et al., 2021a,b). Some of these chemicals, considered emerging pollutants, originate from a variety of sources including pharmaceuticals products, plastics and other industrial and chemical products (Zhao et al., 2018). Although these pollutants exist at low concentrations in wastewater, surface, underground, and drinking, they are persistent in the environment constituting a significant risk to the well-being of ecosystems due to their high toxicity (Elhalil et al., 2017).

Caffeine is considered a persistent and toxic emergent compound frequently found in surface waters (Kosma et al., 2014). It is the principal constituent of some drinks and foods consumed daily such as coffee, tea, energy drinks, coca-cola, and chocolate (Švorc et al., 2012). In addition, considering its psychoactive effects, it is part of some pharmaceutical products (Rostagno et al., 2011).

However, the occurrence of this emerging pollutant in water can originate adverse ecological effects associate with its resistance to natural degradation and its possible harmfulness to aquatic species and human life (Elhalil et al., 2017). Current strategies for treating emerging pollutants include biological processes (Rosal et al., 2010), activated carbon adsorption (Jeirani et al., 2016; Delgado et al., 2019), membrane filtration (Secondes et al., 2014), and chemical treatments such as chlorination (Noutsopoulos et al., 2013), ozonation (Quiñones et al., 2015), and advanced oxidation processes (Souza et al., 2017). In relation to this last methodology, the application of heterogeneous photocatalysis is considered an effective, easy, ecological, profitable, and innovative alternative for the removal of emerging pollutants.

Titanium dioxide (TiO_2) is one of the main semiconductor materials with effective photocatalytic properties in the field of environmental remediation (Murcia et al., 2015) and the generation of clean energy (Chiarello et al., 2017). However, the recombination frequency of charge carriers in the semiconductor is very high, which leads to reduced photoactivities. In order to optimize the photocatalytic properties of the semiconductor, one of the most employed strategies deals with an adjustment in surface and/or structural conditions of the material, which allows reducing electron/hole pair recombination and favors its migration towards the surface (consequently allowing a greater availability of adsorbed species). In this sense, some studies developed in our research group report on the convenience of in-situ modification of TiO_2 with fluoride anions, effective in photocatalytic reduction reactions of nitroaromatic contaminating compounds (Castañeda et al., 2016).

However, the construction of heterojunctions in photocatalytic materials is considered one promising methodology to improve the photocatalytic properties of semiconductors due to its effectiveness for the separation of the charge carriers. For example, Carvalho et al. evaluated caffeine degradation using ZnO:$ZnWO_4$ heterostructures prepared via hydrothermal method. The authors reported negligible photoactivity when the reaction was conducted in the absence of a photocatalyst. The prepared composites showed low pollutant adsorption (<5%) and these were active in the degradation reaction. 3Zn:1ZnW and 1Zn:1ZnW heterostructures were able to completely degrade the pollutant, while, near to 40% of the caffeine was oxidized using ZnO and $ZnWO_4$ materials. The photocatalytic yield was associated to the spontaneous formation of heterojunctions between ZnO and $ZnWO_4$ during the synthesis stage, which increased the useful life of the electron/hole pairs (Carvalho et al., 2019).

Elhalil et al. studied the heterostructure of ZnO–Al_2O_3 doped with different Mg content (1, 3 and 5 wt%) in the degradation reaction of caffeine using ultraviolet radiation. The authors evidenced that the 1% Mg–ZnO–Al_2O_3 photocatalyst presented the major photoactivity and degradation of 98.9% was reached, being significantly higher as compared to pure ZnO and commercial Degussa P-25. The enhanced photoactivity was associated with interfacial heterostructure in the solid (Elhalil et al., 2018).

Tahir et al. evaluated a photocatalyst of WO_3–TiO_2-g-C_3N_4 (WTCN) obtained by the hydrothermal method. This study considered the photodegradation of caffeine using visible light radiation. WTCN photocatalyst demonstrated higher catalytic activity as compared to WO_3 and WO_3/TiO_2. The integration of g-C_3N_4 in the WO_3/TiO_2 compound evidenced an important effect on the photocatalytic yield, obtaining a pollutant removal of around 97%. The improved photocatalytic activity of the WTCN compound can be associated to absorption in the visible region of the electromagnetic spectrum; obtaining a higher surface area and effective charge separation associated with synergistic effects between g-C_3N_4 and WO_3/TiO_2 (Tahir et al., 2019).

On the other hand, coupling an n-type semiconductor such as TiO_2 and a p-type semiconductor that differs in their energy-gap band structure can result in the formation of appropriate band alignments for the effective diffusion of photogenerated electrons and holes during irradiation. As a result, a region of space charge at the interface is formed. The difference in electric potential allows the generation of a strong electric field that accelerates the separation of charge carriers (Ge et al., 2019).

In this work, the synthesis of NiO/TiO_2–F and CuO/TiO_2–F composites materials is proposed and its evaluation in caffeine photocatalytic degradation under UV irradiation. For comparison, unmodified TiO_2 was also studied. Materials were characterized by several techniques in order to identify their physicochemical properties. Reuse tests were subsequently conducted to confirm the stability of the photocatalytic materials.

2. Material and methods

2.1. Synthesis of the photocatalytic composites

Photocatalytic support of fluorinated TiO_2 (1.0% wt) was prepared by *in-situ* fluorination of the semiconductor using a sol-gel method. The percentage of anion was chosen based in previous studies realized in our research group (Castañeda et al., 2018). For this purpose, titanium butoxide was added to butyl alcohol and ammonium fluoride was used as anionic precursor and as hydrolysis catalyst of the synthesis. The precursor mixture was stirred maintaining the temperature at 40 °C for 2 h. Then, 50 mL of ethanol solution were added drop by drop to the initial mixture and the formation of a precipitate was observed. The molar relation of alkoxide:butyl alcohol:water was 1:35:8. The white precipitate obtained was filtered and washed and it was dried at 85 °C for 48 h. Finally, the xerogel was ground and the powder obtained was annealed at 400 °C for 6 h. For comparison, sol-gel pristine TiO_2 was synthesized.

The composites of NiO/TiO_2–F and CuO/TiO_2–F were obtained by wet impregnation of the TiO_2–F support. $Cu(NO_3)_2{\cdot}3H_2O$ and $Ni(NO_3)_2{\cdot}6H_2O$ were used as precursor reactants. In order to obtain composites with metal oxide percentage of 1.0 wt%, the calculated amount de precursor agents were added in two beakers containing a 20 mL of a suspension of the fluorinated support, which was maintained at 80 °C under vigorous stirring. The solids were dried at 85 °C and annealed at 400 °C for 4 h.

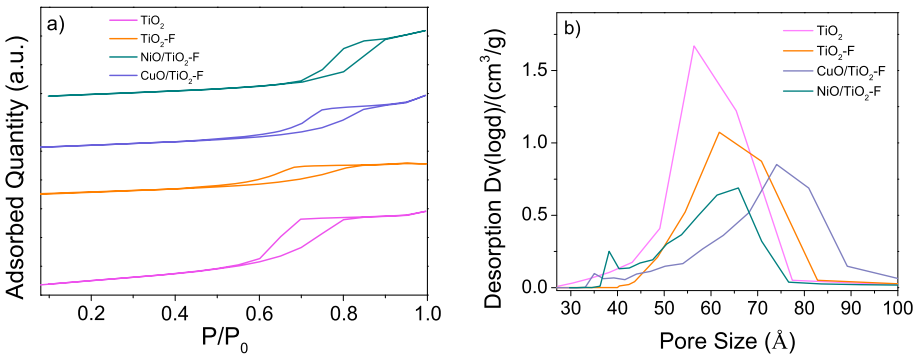

Fig. 1. a) N_2 adsorption-desorption isotherm. **b)** BJH pore size distribution (from the desorption branch of the isotherms).

2.2. Characterization of the photocatalytic composites

Elemental analysis of Ni and Cu present in the composites was evaluated by X-ray fluorescence spectroscopy using a JSX-1000S spectrophotometer.

Nitrogen adsorption-desorption isotherms of the composites were measured using a Micromeritics ASAP 2020 analyzer. Materials were previously evacuated at 250 °C for 4 h. BET and BJH methods were considered to estimate the textural properties such as surface area and pore size of the solids.

Crystalline phase and crystallite size of the composites were studied by X-ray diffraction. The diffraction patterns were collected employing a Bruker D2 Phaser diffractometer. The measurements were recorded using Cu Kα radiation in the 2θ range from 10 to 80° and a step of 0.02°.

High resolution transmission electron microscopy (HRTEM) was carried out in a field emission transmission electron microscope, JEM-2200FS with a resolution of 0.1 nm and operated at 200 kV.

UV–Vis diffuse reflectance spectra were collected using a Varian Cary 100 spectrophotometer with integration sphere in a scanning range of 200–700 nm $BaSO_4$ was employed as reference standard.

X-ray photoelectron spectroscopy analysis were realized using a VG Scientific ESCALAB 250 spectrometer. This equipment is equipped with a hemispherical electron analyzer and an X-ray source with monochromatic Al K_α radiation (hv = 1486.6 eV). Prior the analysis, the samples were embedded onto indium foils which were pressed manually and placed to a holder.

2.3. Caffeine photocatalytic degradation

The photocatalytic behavior of the composites and the fluorinated support was evaluated in the photocatalytic degradation of caffeine as a test molecule. A high-pressure mercury lamp emitting at 254 nm, 4.4 mW UV was employed as irradiation source. Experiments were conducted using a glass reactor coupled with a water jacket, which let to keep a constant temperature during the photocatalytic reaction. Tests were performed by adding 200 mL of a 25 ppm caffeine solution and 100 mg of photocatalytic material. In order to favor adsorption/desorption equilibrium, the suspension was maintained under vigorous stirring at 800 rpm, with constant bubbling of air, in the dark for 30 min. Irradiation was subsequently initialized and aliquots were taken out every 30 min during 3 h of reaction. Samples were withdrawn, filtered and caffeine concentration was monitored by Evolution 300 UV–Vis spectrophotometer. The estimation of the residual total organic carbon was performed using a TOC/TN analyzer multi N/C 2100.

3. Results and discussion

3.1. Characterization of the photocatalytic composites

CuO and NiO content in the composites was calculated from quantification of the metals by X-ray fluorescence analysis. The contents estimated of the metal oxides were 0.92 and 0.89 wt% for the CuO/TiO_2–F and NiO/TiO_2–F composites, respectively, slightly lower than nominal load (corresponding to 1.0 wt%).

Table 1
Physicochemical parameters of the studied materials.

Photocatalyst	S_{BET} (m^2/g)	Pore size (Å)	Crystallite size (nm)	Eg (eV)
TiO_2	126	56	10.1	3.01
TiO_2–F	64	62	12.2	2.98
NiO/TiO_2–F	63	66	12.0	2.99
CuO/TiO_2–F	64	74	11.4	2.79

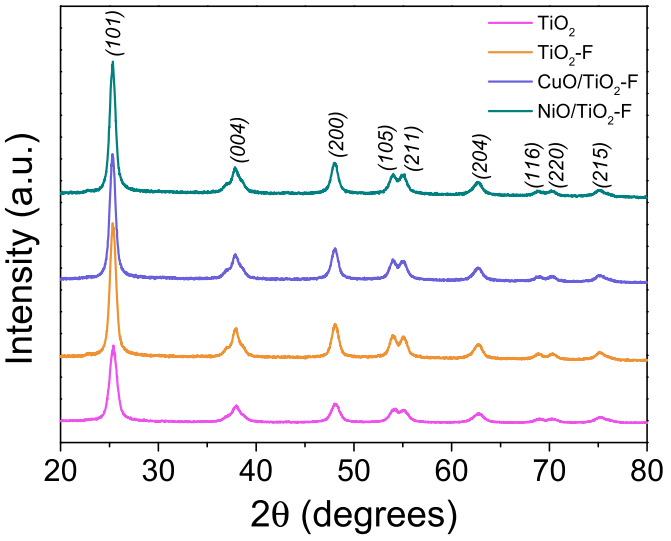

Fig. 2. X-ray diffraction patterns of the photocatalytic materials.

N_2 adsorption-desorption isotherms of the photocatalysts are shown in Fig. 1 a). All solids evidenced type IV isotherms, characteristic of mesoporous materials with a H2 hysteresis loop associated to ink-bottle pores (Mahu et al., 2021). BJH pore size distributions from the desorption branch of the isotherms are presented in Fig. 1 b). Pore density decreases with fluorination and subsequently with CuO or NiO deposition. Taking a closer look at the pore size distribution of the samples (Fig. 1b), the formation of pores with lowest size is most evident with CuO or NiO. This can be consequence of the non-uniform deposition of these oxides on TiO_2–F or the associated porosity contribution.

Textural properties of the materials corresponding to surface area and pore size are listed in Table 1. As previously reported (Castañeda et al., 2016), *in-situ* fluorination of TiO_2 causes an important decrease in surface area, which seems to be related to an increase in crystallite size.

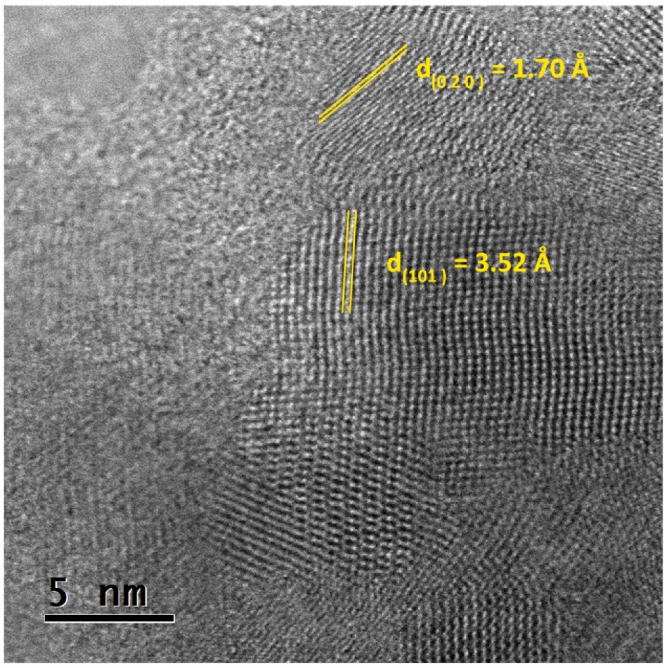

Fig. 3. HRTEM characterization of the heterojunction in CuO/TiO_2–F composite.

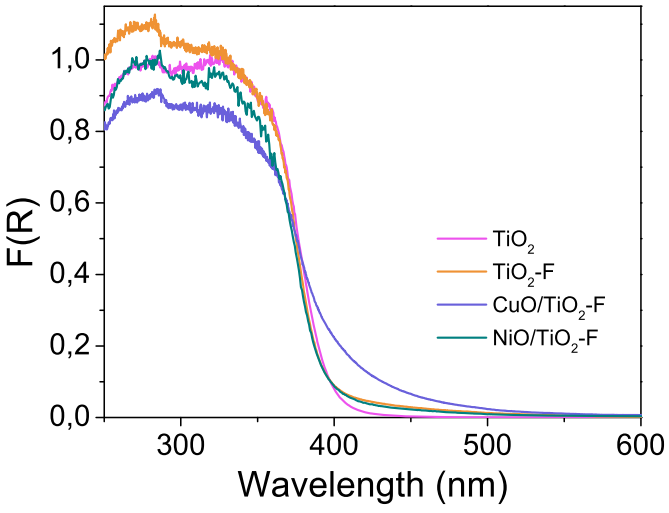

Fig. 4. UV-DRS spectra of the photocatalytic materials.

However, the incorporation of NiO and CuO on fluorinated support did not change any textural properties, suggesting similar crystalline characteristics.

Fig. 2 shows the X-ray diffraction patterns of TiO_2, fluorinated support, NiO/TiO_2–F and CuO/TiO_2–F composites. The characteristic diffraction signals of the anatase polymorph of TiO_2 could be easily identified (Singh, 2017). The low contents of the metal oxides impregnated on the fluorinated semiconductor did not allow the identification of CuO located at $2\theta = 35.7°$ (Khemthong et al., 2013) or those of NiO at $2\theta = 43.3°$ (Uddin et al., 2017). Diffraction peaks in all samples are strong and sharp, suggesting that the solids are highly crystalline (Bellardita et al., 2018).

Crystallite sizes were calculated using the Debye-Scherrer equation from the broadening of the diffraction peak located at $2\theta = 25.4°$ associated to the plane (101) of the anatase phase of titanium dioxide. Values obtained are indicated in Table 1. The estimated crystallite size for TiO_2 is 10.1 nm, with fluorination promoting the growth of anatase crystallites (Table 1, 12.2 nm; Castañeda et al., 2016). In relation to composite materials, a slight decrease in this structural parameter was evidenced. This result suggests the existence of a strong interaction between the particles of metal oxides CuO and NiO with TiO_2–F (Zeng et al., 2017).

HRTEM studies were subsequently performed for CuO/TiO_2–F (Fig. 3). The phases TiO_2–F and CuO could be identified by the differences in lattice parameters. Interplanar distances equal to 1.70 Å are associated to crystalline planes (020) of CuO while lattice spacing equal to 3.52 Å corresponds to (101) TiO_2–F planes. Both phases are in an intimate contact at the separating interface suggesting the formation of heterojunctions. It is known that the junction between a type-p semiconductor (CuO) and a type-n semiconductor (TiO_2–F) could promote the effective separation of charge carriers, enhacing the photoactivity of the material (Shi et al., 2018).

UV–Vis diffuse reflectance spectra of TiO_2–F support as well as NiO/TiO_2–F and CuO/TiO_2–F are presented in Fig. 4. As it can be seen, all of these materials display the characteristic absorption of anatase polymorph of TiO_2 with an intense band the UV region. As it is well known, in the TiO_2 semiconductor, the valence band is formed of O_{2p} states and the conduction band is formed of Ti_{3d} states (Nagao et al., 2010). The absorption band around to 350 nm is due to $O_{2p} \rightarrow Ti_{3d}$ electronic transition (Lv et al., 2012). A weak shoulder in the region from 250 to 300 nm is associated to electron transfer from the ligand-oxygen to an unoccupied orbital of the tetracoordinated titanium of the lattice (Petkowicz et al., 2010; Montañez et al., 2015; Castañeda et al., 2018). TiO_2–F and NiO/TiO_2–F composite evidence similar behavior, however, the absorption edge of CuO/TiO_2–F presents a slight red-shift. The absorption at higher wavelengths suggests a faster generation rate of charge carriers on the photocatalyst surface (Liu and Zhou, 2015).

Band gap energy (*Eg*) values were estimated from a plot of modified Kubelka-Munk equation $[F(R) \times h\nu]^{1/2}$ in function of absorbed light energy ($h\nu$) (not showed) considering allowed indirect transitions of TiO_2 and these are listed in Table 1. *In-situ* fluorination of the semiconductor promotes a slight decrease in band gap, which could be related with the insertion of fluoride anion in the lattice of the semiconductor and the possible generation of Ti^{3+} species, as previously reported (Castañeda et al., 2016). On the other hand, NiO/TiO_2–F composite presents a bang gap energy very similar to TiO_2–F and as expected, CuO/TiO_2–F composite evidenced a band gap value slightly lower, which could be a result of the narrow *Eg* of the copper oxide (1.2 eV).

High resolution spectra of Ti 2p, O 1s and F 1s of the solids studied are presented in Fig. 5 a). Two signals located at 464.7 eV and 458.9 eV are observed in the Ti 2p spectrum, which are associated to Ti $2p_{1/2}$ and Ti $2p_{3/2}$, respectively. This doublet corresponds to Ti^{4+} ions in the TiO_2 lattice (Castañeda et al., 2016; Sacco et al., 2020). The presence of a third signal at 460 eV in TiO_2–F is corresponding to Ti^{3+} $2p_{1/2}$ (Bharti et al., 2016) which is associated with the substitution of F^- ions in the lattice TiO_2, which localize the extra electron needed for charge compensation (Czoska et al., 2008). In fact, the principal signal located at 684.4 eV in the F 1s region (Fig. 5b) is representative of surface fluoride species in ≡Ti–F bonds, while the small contribution at 687.5 eV is associated to fluoride species substituting oxygen sites in lattice of TiO_2 (Ti–F–Ti) (Castañeda et al., 2016).

It is worth mentioning that the signals associated with Ti^{3+} were not evidenced in the spectrum of CuO/TiO_2–F which could be related to a low concentration of these species to be detected by XPS analysis. However, this signal remains in NiO–TiO_2–F, again confirming the distinct interaction of CuO or NiO on TiO_2–F. This could be correlated with O 1s spectra. Generally, the signals associated to O 1s (Fig. 5 c) are deconvoluted into two contributions thus: a signal centered to 532.1 eV associated to chemisorbed oxygen and a second signal located at 530.1 eV corresponding to the lattice oxygen (Vignesh et al., 2020). The proportion of these signals changes with the incorporation of CuO or NiO.

CuO/TiO_2–F present a highest proportion of species oxygen

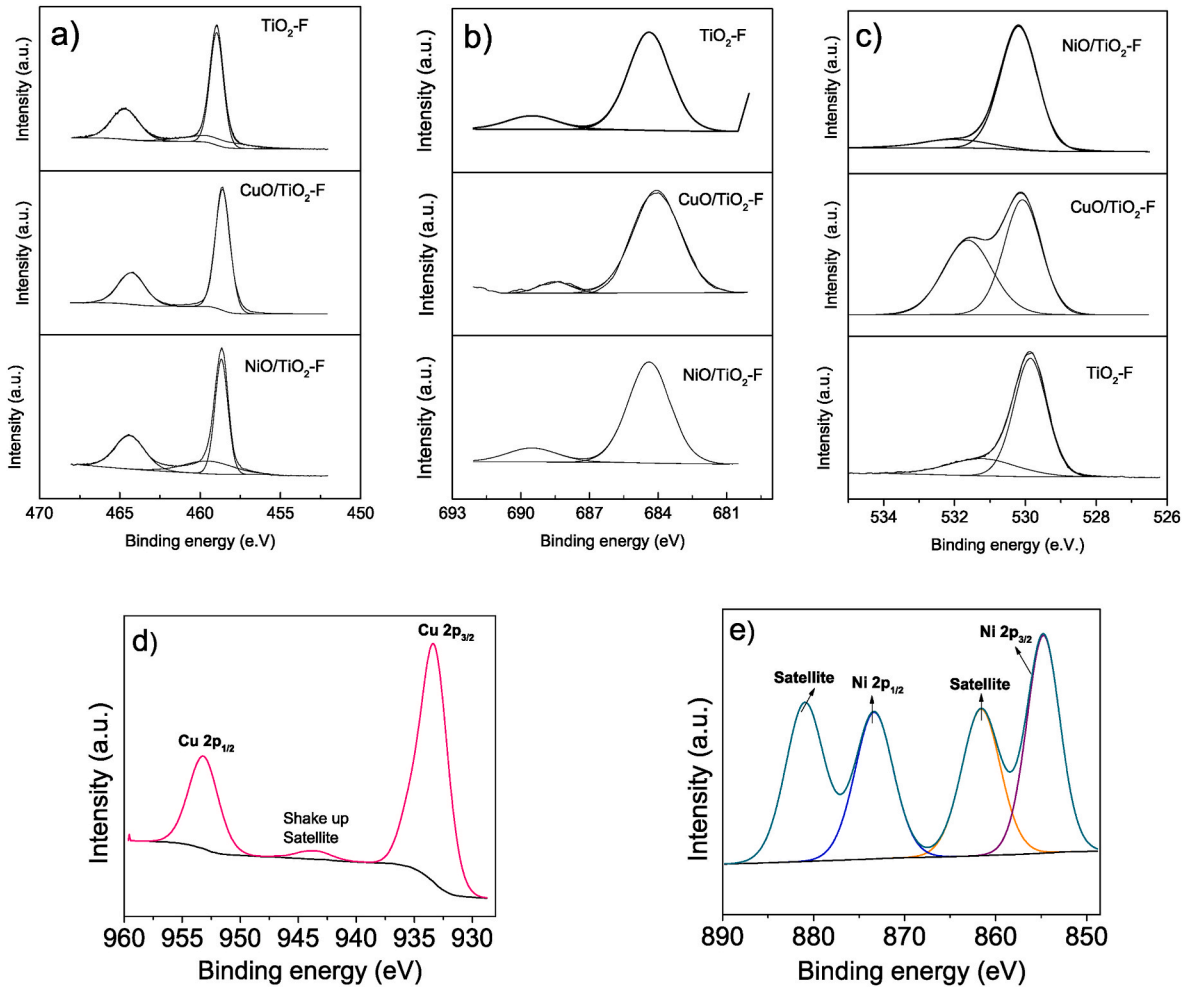

Fig. 5. High resolution spectra of the TiO_2–F support: (a) Ti 2p, (b) O 1s, (c) F 1s. High resolution spectra of (d) Cu 2p for the CuO/TiO_2–F and (e) Ni 2p for the NiO/TiO_2–F photocatalysts.

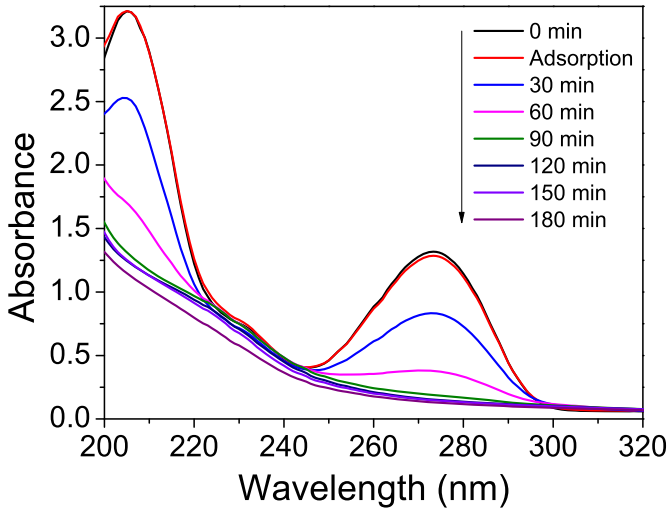

Fig. 6. UV absorption spectra of caffeine degradation as a function of reaction time using CuO/TiO_2–F.

chemisorbed (absence of Ti^{3+} peaks), while NiO/TiO_2–F preserve Ti^{3+} peaks but decrease the proportion of chemisorbed oxygen species. These results are in good agrement with the diffuse reflectance results and N_2-physisorption. A highest segregation of CuO species as compared to NiO on the surface of TiO_2–F is present, increasing defect sites and consequently decreasing the band gap. Defect sites are commonly associated with chemisorbed oxygen (El-Atab et al., 2016).

On the other hand, in Fig. 5 d) is presented the high-resolution spectrum of Cu 2p of the CuO/TiO_2–F composite material. As can be seen, the two representative contributions of copper in oxidative state 2^+ are observed at 953.3 and 933.4 eV which corresponding to Cu $2p_{1/2}$ and Cu $2p_{3/2}$, respectively. Besides, a shake-up satellite signal is observed in range from 940 to 946 eV which is related to the charge transfer transitions from the O^{2-} ions into the unfilled valence level (d^9) of the Cu^{2+} ion (Castañeda et al., 2018).

For NiO/TiO_2–F, a characteristic doublet with its respective satellite peak of nickel in the Ni 2p region could be found (Fig. 5 e). In this sense, the main signals of Ni $2p_{1/2}$ and Ni $2p_{3/2}$ were observed at 873.3 and 854.7 eV, respectively, associated to Ni^{2+} cation, in good agreement with information reported in literature (Uddin et al., 2017).

3.2. Caffeine photocatalytic degradation

Fig. 6 shows changes in the UV absorption spectra of caffeine at different times of irradiation in the presence of CuO/TiO_2–F. UV absorption spectra of caffeine show a pair of main absorption bands at 205 nm and 273 nm, associated with electronic transitions $\pi \rightarrow \pi^*$ and $n \rightarrow \pi^*$, respectively (Gómez et al., 2020). As the reaction progresses, there is a significant decrease in the intensities of the absorption bands, which suggests the degradation of the emerging pollutant. The same absorption

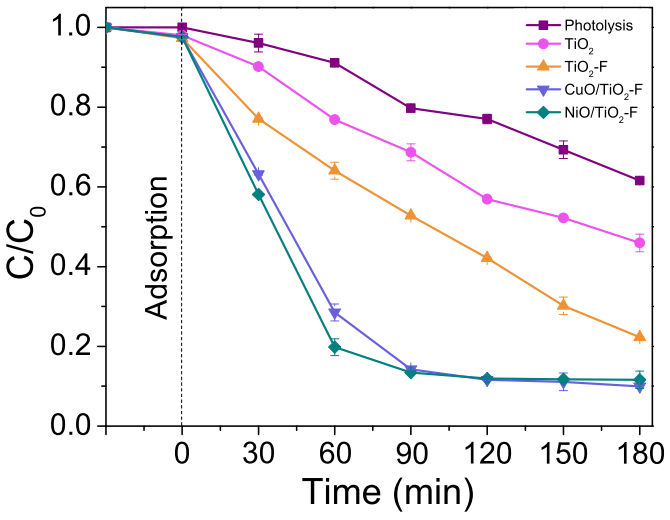

Fig. 7. Variation of the relative concentration of caffeine as a function of time using the materials studied.

bands were evidenced in the spectra obtained using the other materials studied and in the absence of photocatalyst.

The variation of the relative concentration of caffeine as a function of the reaction time is indicated in Fig. 7. During photolysis tests (in the absence of photocatalyst), a degradation of 38% was reached, which suggests that the radiation alone could lead to oxidation of the pollutant. The degradation of the molecule depends on its ability to absorb the given radiation and reach an excited state, leading to bond breaking. If the molecule is not directly degraded by photolysis, then indirect degradation caused by the formation of hydroxyl radicals from water can take place (Nawaz and Sengupta, 2019).

After 180 min of irradiation, caffeine degradation was equal to 54 and 78% using TiO_2 and TiO_2–F, respectively. Importantly, the reactions conducted in presence of CuO/TiO_2–F and NiO/TiO_2–F composites showed an efficiency of 90 and 88%, respectively. Based on these results, the *in-situ* fluorination of TiO_2 had a positive effect on the photocatalytic properties of the semiconductor, reflected in an increase in photoactivity and effectiveness in the degradation process of the pollutant. As could be evidenced by XPS analysis, the modification of titanium dioxide with fluoride anions using the sol-gel synthesis method leads to the generation of two types of fluorine species in the solid, namely fluoride ions

Table 2
Kinetic parameters for the photocatalytic degradation of caffeine.

Photocatalyst	$k \times 10^{-3}(M/min)$	$t_{1/2}(min)$	R^2
TiO_2	4.53	153	0.980
TiO_2–F	6.84	101	0.998
CuO/TiO_2–F	19.1	36	0.962
NiO/TiO_2–F	18.9	37	0.901

replacing oxygen sites in the TiO_2 lattice (Ti–F–Ti) as well as forming bonds on the surface of the material with titanium species (≡Ti–F). Possibly, ≡Ti–F species attract photogenerated electrons to the surface of the semiconductor due to the high electronegativity of the anion, which favors a decrease in the recombination frequency of the electron-hole pair and thus increasing the availability of the holes for the generation of hydroxyl radicals (•OH), the main responsible for the degradation of organic pollutants (Deng et al., 2017; Castañeda et al., 2021). Regarding the photocatalytic behavior of the composite materials, a significant increase in photoactivity could be evidenced, compared to that obtained using TiO_2–F. The presence of NiO and CuO could favor the development of p-n heterojunctions that promote electron transfer and effective separation of charge carriers.

The p-n semiconductor heterojunction system is an efficient design for the separation of charge carriers. Thus, when the p-type and n-type semiconductors are in contact, they originate the p-n junction, in which a region of interfacial space charge is formed, as a consequence of the diffusion of electrons (from the n-type to the p-type semiconductor) and holes (from the p-type to the n-type semiconductor). Once the p-n heterojunction is irradiated with energy higher or equal than the forbidden bands of the photocatalysts, photogenerated electron-hole pairs can be rapidly separated by the electric field incorporated within the region of space charge. Electrons are then transferred to the conduction band of the n-type semiconductors impulse by the electric field, and the holes to the valence band of the p-type semiconductors, achieving an effective separation of the charge carriers (Fig. 8).

From photoactivity results, the degradation of caffeine follows a first-order kinetics. The kinetic parameters including the apparent rate constants (k), half-life time ($t_{1/2}$) as well as the statistical coefficient (R^2) are summarized in Table 2.

Results obtained suggest that the use of CuO/TiO_2–F and NiO/TiO_2–F favor an increase in the rate of the reaction, being 4.2 and 2.8 times higher than that obtained with TiO_2 and TiO_2–F photocatalytic support, respectively.

The percentage of residual total organic carbon (TOC) in the solution

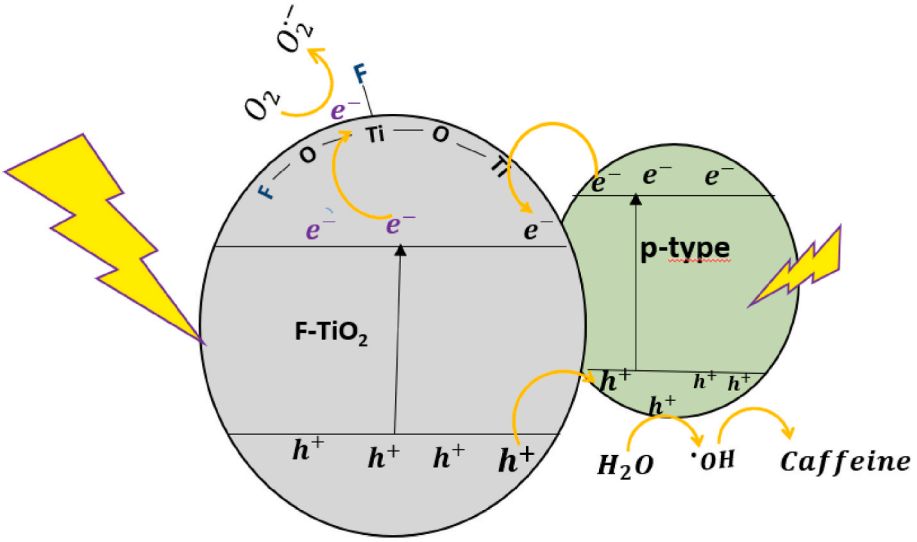

Fig. 8. Representation of the charge transference in the compound materials used in caffeine photocatalytic degradation.

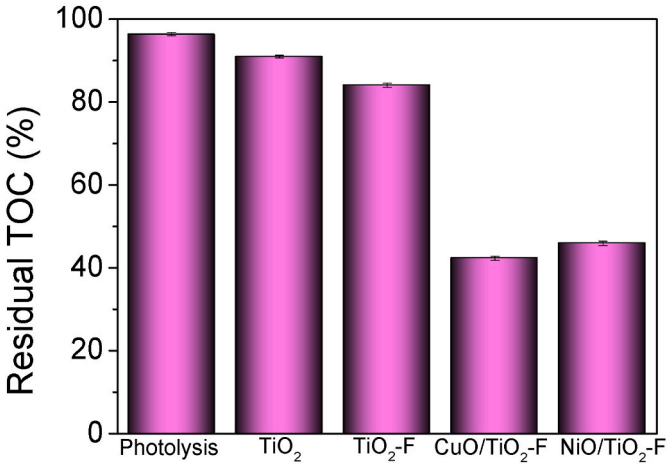

Fig. 9. Percentage of residual TOC of the photocatalytic degradation of caffeine.

after 180 min of photocatalytic reaction is presented in Fig. 9.

These results demonstrate that composite materials are most efficient in caffeine photodegradation, achieving a removal of the emerging contaminant of 58% and 54%, using CuO/TiO_2–F and NiO/TiO_2–F, respectively. High residual TOC values obtained when the reaction is conducted in the presence of TiO_2 and the fluorinated support TiO_2–F confirm that the degradation of the contaminant is poorly effective. This difference is commonly encountered in distinct catalytic systems and suggested the formation of byproducts that cannot be completely mineralized. Caffeine is almost completely degraded but generates persistent organic intermediates resistant to further oxidations. In our system, the generations of hydroxyl radicals (see results above) are involved in the degradation of caffeine as well accepted by theoretical studies and experimental studies that this type of radicals form a C8–OH radical adduct forming 8-oxocaffeine and posteriorly 1,3,7-trimethyluric acid as major sideproducts (Stadler et al., 1996; Telo and Vieira, 1997). These byproducts exhibited similar ecotoxicity to that of caffeine, but caffeine has a potential hazard to ecosystems and human health due to its uncontrolled emissions (Li et al., 2021a,b).

With these premises, the fluorination of TiO_2 is believed to have an important effect on the photocatalytic activity of the semiconductor: regulating its physical and chemical properties including crystallite size, surface area and band gap energy as well as fluorine species bound to the surface promoting a decrease in the recombination of electron-hole pairs, indispensable to improve the contaminant degradation process. p-n heterojunctions originated from the coupling of the fluorinated semiconductor with CuO and NiO, potentiate the separation of electrons and photogenerated holes and significantly improve the photocatalytic activity in caffeine degradation reaction.

3.3. Study of the production of •OH radicals

In order to verify •OH radicals production, the main oxidative agent in photodegradation reactions, fluorescence analysis were finally conducted. Terephthalic acid was employed as trapping agent of hydroxyl radicals due to formation of 2-hydroxyterephthalic (TAOH) acid, which is easily identified by its emission wavelength at 425 nm (Castañeda

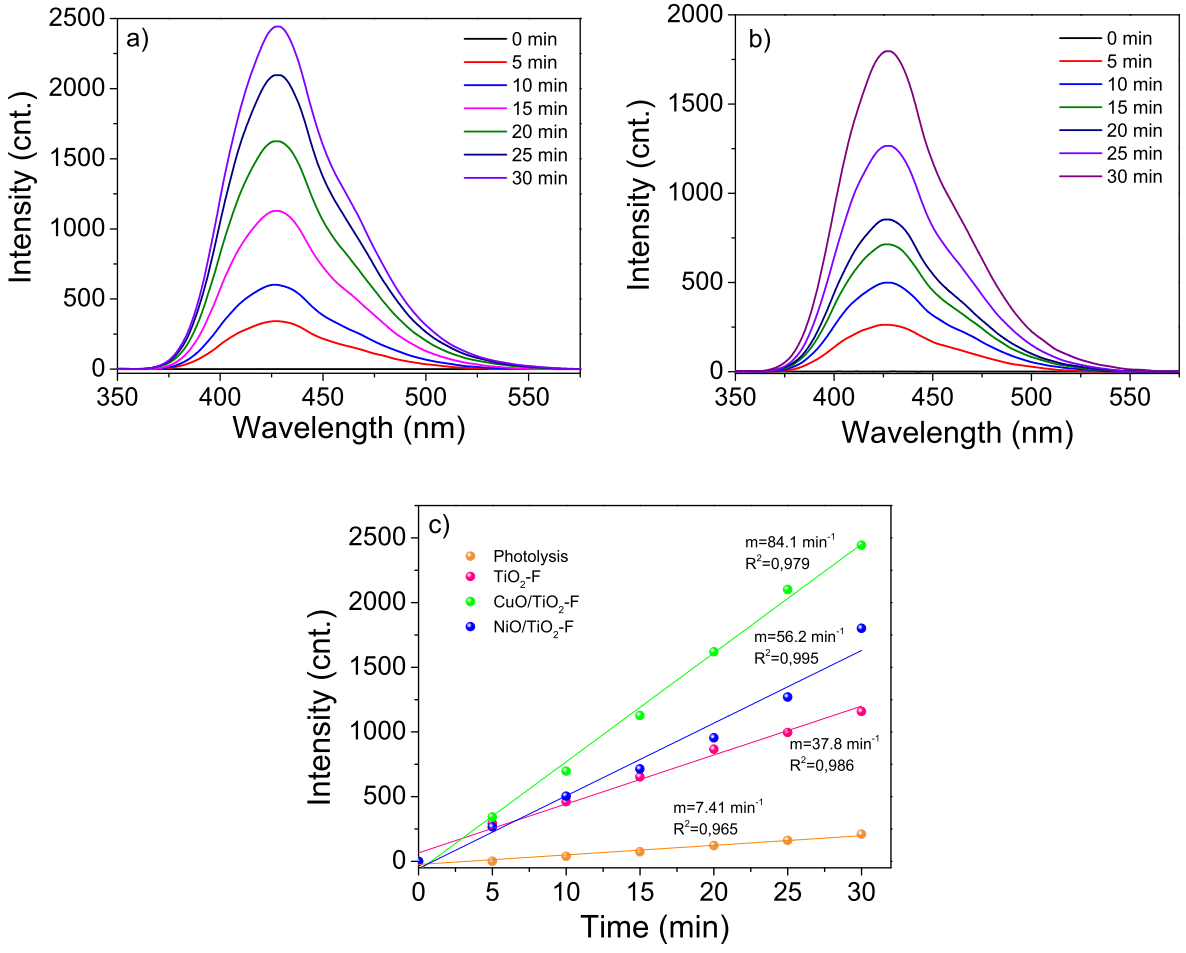

Fig. 10. 2-Hydroxyterephthalic acid fluorescence spectra of: a) CuO/TiO_2–F, b) NiO/TiO_2–F. c) Profile of linear rate of •OH radical production.

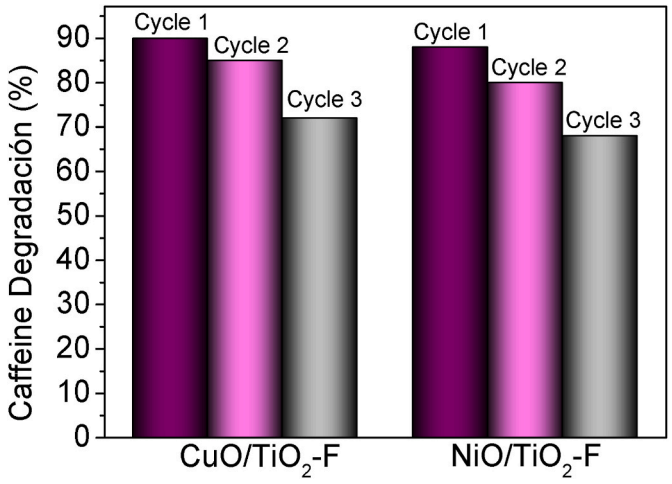

Fig. 11. Degradation percentages using CuO/TiO_2–F and NiO/TiO_2–F (three reuses).

et al., 2018).

Fig. 10 a-b) shows the fluorescence spectra of 2-hydroxyterephthalic acid using CuO/TiO_2–F and NiO/TiO_2–F photocatalysts. The intensity of the signal at 425 nm increases with the advance of the reaction, suggesting an increase in •OH radicals formation during the photocatalytic process as consequence of the generation of TAOH. Besides, the generation rate of hydroxyl radicals is favored in presence of these two types of solids as evidenced in Fig. 10 c). CuO/TiO_2–F and NiO/TiO_2–F exhibited a rate of hydroxyl radical generation 2.2 and 1.5 higher than that achieved using TiO_2–F.

If well the fluorination of TiO_2 has an important influence on the photoactivity of TiO_2, the p-n heterojunctions originated from the coupling of the fluorinated semiconductor with CuO and NiO potentiate the separation of photogenerated e^-/h^+ pairs, increasing holes availability for the generation of hydroxyl radicals ($^{\bullet}OH$); thus, a significant improvement in the degradation process of the emerging pollutant was achieved.

3.4. Reuse of the composites materials in the caffeine photocatalytic degradation

In order to evaluate the stability of NiO/TiO_2–F and CuO/TiO_2–F photocatalysts, reuse tests were carried out for three cycles under otherwise identical experimental conditions (Fig. 11). After 180 min of reaction, the solids were separated from solution and washed with distilled water, then dispersed in a fresh aqueous caffeine solution. After three (3) reuse tests, CuO/TiO_2–F material did not show a significant loss of activity and a caffeine degradation of 90, 85 and 72% was achieved, respectively. A similar behavior was evidenced for NiO/TiO_2–F, with a degradation of 88, 80 and 68% obtained after subsequent cycles.

4. Conclusions

The effect of CuO and NiO addition on TiO_2–F support was assessed in the photocatalytic degradation of caffeine under UV irradiation. The physicochemical characterization of the samples was studied by several techniques. In particular, a change in textural and structural properties was promoted via fluorination of TiO_2. The generation of surface ≡Ti–F species favors an increase in photoactivity. However, the degradation of the emerging pollutant was notably enhanced using CuO/TiO_2–F and NiO/TiO_2–F composite materials, which could be result of the formation of heterojunctions responsible for improvements in the separation of charge carriers and therefore of the observed increase in caffeine photodegradation.

Author Contribution Statement

The authors confirm contribution to the paper as follows: conceptualization, C.C, J.J.M, R.L; methodology, C.C, LS.; investigation, L.S, C. C, J.J.M, S.M.O, R.G, H.R, ; resources, data curation, C.C, J.J.M, R.G, R. L.; writing—original draft preparation, C.C, J.J.M; writing—review and editing, R.G, R.L; supervision, R.G, ; project administration, C.C, J.J.M, R.L, S.M.O, funding acquisition, H.R. J.J.M, S.M.O, R.L. All authors have read and agreed to the published version of the manuscript.

Declaration of competing interest

The authors declare that they have no known competing financial interests or personal relationships that could have appeared to influence the work reported in this paper.

Acknowledgments

This paper has been supported by RUDN University Strategic Academic Leadership Program (R. Luque). This project was funded by the Researchers Supporting Project number (RSP-2021/405), King Saud University, Riyadh, Saudi Arabia. J.J.M wishes to thank the Vicerrectoría de Investigaciones (Project SGI 3055) from Universidad Pedagógica y Tecnológica de Colombia for financial support.

References

Bharti, B., Kumar, S., Lee, H.N., Kumar, R., 2016. Formation of oxygen vacancies and Ti^{3+} state in TiO_2 thin film and enhanced optical properties by air plasma treatment. Sci. Rep. 6, 1–12.

Bellardita, M., Di Paola, A., Megna, B., Palmisano, L., 2018. Determination of the crystallinity of TiO_2 photocatalysts. J. Photochem. Photobiol., A 367, 312–320.

Carvalho, K.T.G., Lopes, O.F., Ferreira, D.C., Ribeiro, C., 2019. ZnO:$ZnWO_4$ heterostructure with enhanced photocatalytic activity for pollutant degradation in liquid and gas phases. J. Alloys Compd. 797, 1299–1309.

Castañeda, C., Tzompantzi, F., Gómez, R., 2016. Photocatalytic reduction of 4-nitrophenol on in situ fluorinated sol–gel TiO_2 under UV irradiation using Na_2SO_3 as reducing agent. J. Sol. Gel Sci. Technol. 80, 426–435.

Castañeda, C., Tzompantzi, F., Rodríguez-Rodríguez, A., Sánchez-Dominguez, M., Gómez, R., 2018. Improved photocatalytic hydrogen production from methanol/water solution using CuO supported on fluorinated TiO_2. J. Chem. Technol. Biotechnol. 93, 1113–1120.

Castañeda, C., Alvarado, I., Rojas, H., Tzompantzi, F.J., Gomez, R., 2021. Photocatalytic degradation of the 2,4-dichlorophenoxyacetic acid herbicide using supported iridium materials. Ciencia en Desarrollo 12, 125–134.

Chiarello, G.L., Dozzi, M.V., Selli, E., 2017. TiO_2-based materials for photocatalytic hydrogen production. J. Energy. Chem. 26, 250–258.

Czoska, A.M., Livraghi, S., Chiesa, M., Giamello, E., Agnoli, S., Granozzi, G., Finazzi, E., Di Valentin, C., Pacchioni, G., 2008. The nature of defects in fluorine-doped TiO_2. J. Phys. Chem. C 112, 8951–8956.

Delgado, N., Capparelli, A., Navarro, A., Marino, D., 2019. Pharmaceutical emerging pollutants removal from water using powdered activated carbon: study of kinetics and adsorption equilibrium. J. Environ. Manag. 236, 301–308.

Deng, X., Zhang, H., Ma, Q., Cui, Y., Cheng, X., Li, X., Xie, M., Cheng, Q., 2017. Fabrication of p-NiO/n-TiO_2 nano-tube arrays photoelectrode and its enhanced photocatalytic performance for degradation of 4-chlorphenol. Separ. Purif. Technol. 186, 1–9.

El-Atab, N., Chowdhury, F., Ulusoy, T.G., Ghobadi, A., Nazirzadeh, A., Okyay, A.K., Ammar, Nayfeh, 2016. ~3-nm ZnO nanoislands deposition and application in charge trapping memory grown by single ALD step. Sci. Rep. 6, 1–11.

Elhalil, A., Elmoubarki, R., Farnane, M., Machrouhi, A., Sadiq, M., Mahjoubi, F.Z., Qourzal, S., Barka, N., 2018. Photocatalytic degradation of caffeine as a model pharmaceutical pollutant on Mg doped ZnO-Al_2O_3 heterostructure. Environ. Nanotechnol. Monit. Manag. 10, 63–72.

Elhalil, A., Elmoubarki, R., Machrouhi, A., Sadiq, M., Abdennouri, M., Qourzal, S., Barka, N., 2017. Photocatalytic degradation of caffeine by ZnO-$ZnAl_2O_4$ nanoparticles derived from LDH structure. J. Environ. Chem. Eng. 5, 3719–3726.

Ge, J., Zhang, Y., Heo, Y.J., Parket, S.J., 2019. Advanced design and synthesis of composite photocatalysts for the remediation of wastewater: a review. Catalysts 9, 122–154.

Gómez, S., Giovannini, T., Cappelli, C., 2020. Absorption spectra of xanthines in aqueous solution: a computational study. Phys. Chem. Chem. Phys. 22, 5929–5941.

Jeirani, Z., Niu, C., Soltan, J., 2016. Adsorption of emerging pollutants on activated carbon. Rev. Chem. Eng. 33, 491–522.

Khemthong, P., Photai, P., Grisdanurak, N., 2013. Structural properties of CuO/TiO_2 nanorod in relation to their catalytic activity for simultaneous hydrogen production under solar light. Int. J. Hydrogen Energy 38, 15992–16001.

Kosma, C.I., Lambropoulou, D.A., Albanis, T.A., 2014. Investigation of PPCPs in wastewater treatment plants in Greece: occurrence, removal and environmental risk assessment. Sci. Total Environ. 466–467, 421–438.

Li, M., Mei, Q., Han, D., Wei, B., An, Z., Cao, H., Xie, J., He, M., 2021a. The roles of HO•, ClO• and BrO• radicals in caffeine degradation: a theoretical study. Sci. Total Environ. 768, 1–10.

Li, S.H., Qi, M.Y., Tang, Z.R., Xu, Y.J., 2021b. Nanostructured metal phosphides: from controllable synthesis to sustainable catalysis. Chem. Soc. Rev. 50, 7539–7586.

Liu, Z., Zhou, C., 2015. Improved photocatalytic activity of nano CuO-incorporated TiO_2 granules prepared by spray drying. Prog. Nat. Sci.: Math. Intel. 25, 334–341.

Lv, K., Lv, K., Hu, J., Li, X., Li, M., 2012. Cysteine modified anatase TiO_2 hollow microspheres with enhanced visible-light-driven photocatalytic activity. J. Mol. Catal. Chem. 356, 78–84.

Mahu, E., Coromelci, C.G., Lutic, D., Asaftei, I.V., Sacarescu, L., Harabagiu, V., Ignat, M., 2021. Tailoring mesoporous titania features by ultrasound-assisted sol-gel technique: effect of surfactant/titania precursor weight ratio. Nanomaterials 11, 1–15.

Montañez, J.P., Gómez, S., Santiago, A.N., Pierella, L.B., 2015. TiO_2 supported on HZSM-11 zeolite as efficient catalyst for the photodegradation of chlorobenzoic acids. J. Braz. Chem. Soc. 26, 1191–1200.

Murcia, J.J., Hidalgo, M.C., Navío, J.A., Araña, J., Doña-Rodríguez, J.M., 2015. Study of the phenol photocatalytic degradation over TiO_2 modified by sulfation, fluorination, and platinum nanoparticles photodeposition. Appl. Catal. B Environ. 179, 305–312.

Nagao, Y., Yoshikawa, A., Koumoto, K., Kato, T., Ikuhara, Y., Ohta, H., 2010. Experimental characterization of the electronic structure of anatase TiO_2: thermopower modulation. Appl. Phys. Lett. 97, 172112-172112.

Nawaz, T., Sengupta, S., 2019. Chapter 4 - contaminants of emerging concern: occurrence, fate, and remediation. In: Ahuja, S. (Ed.), Advances in Water Purification Techniques. Elsevier, pp. 67–114.

Noutsopoulos, C., Mamais, D., Thomaidis, N., Koumaki, E., Nika, M., Bletsou, A., Stasinakis, A., 2013. Removal of Emerging Pollutants through Wastewater Disinfection, pp. 1–9.

Petkowicz, D.I., Pergher, S.B.C., Silva da Silva, C.D., Novais da Rocha, Z., Dos Santos, J. H.Z., 2010. Catalytic photodegradation of dyes by in situ zeolite-supported titania. Chem. Eng. J. 158, 505–512.

Quiñones, D.H., Álvarez, P.M., Rey, A., Contreras, S., Beltrán, F.J., 2015. Application of solar photocatalytic ozonation for the degradation of emerging contaminants in water in a pilot plant. Chem. Eng. J. 260, 399–410.

Rosal, R., Rodríguez, A., Perdigón-Melón, J.A., Petre, A., García-Calvo, E., Gómez, M.J., Agüera, A., Fernández-Alba, A.R., 2010. Occurrence of emerging pollutants in urban wastewater and their removal through biological treatment followed by ozonation. Water Res. 44, 578–588.

Rostagno, M.A., Manchón, N., D'Arrigo, M., Guillamón, E., Villares, A., García-Lafuente, A., Ramos, A., Martínez, J.A., 2011. Fast and simultaneous determination of phenolic compounds and caffeine in teas, mate, instant coffee, soft drink and energetic drink by high-performance liquid chromatography using a fused-core column. Anal. Chim. Acta 685, 204–211.

Sacco, O., Murcia, J.J., Lara, A.E., Hernández-Laverde, M., Rojas, H., Navío, J.A., Hidalgo, M.C., Vaiano, V., 2020. Pt–TiO_2–Nb_2O_5 heterojunction as effective photocatalyst for the degradation of diclofenac and ketoprofen. Mater. Sci. Semicond. Process. 107, 104839–104852.

Secondes, M.F.N., Naddeo, V., Belgiorno, V., Ballesteros, F., 2014. Removal of emerging contaminants by simultaneous application of membrane ultrafiltration, activated carbon adsorption, and ultrasound irradiation. J. Hazard Mater. 264, 342–349.

Singh, P.K., 2017. Influence of precursor type on structural, morphological, dielectric and magnetic properties of TiO_2 nanoparticles. Cerâmica 63, 549–556.

Shi, Q., Ping, G., Wang, X., Xu, H., Li, J., Cui, J., Abroshan, H., Ding, H., Li, G., 2018. CuO/TiO_2 heterojunction composites: an efficient photocatalyst for selective oxidation of methanol to methyl formate. J. Mater. Chem. A. 7, 1–8.

Souza, F., Carvalho, C., Féris, L., 2017. Comparison of different advanced oxidation processes for the removal of emerging contaminants in aqueous solutions, 1, 1–4.

Stadler, R.H., Welti, D.H., Stampfli, A.A., Fay, L.B., 1996. Thermal decomposition of caffeic acid in model systems: identification of novel tetraoxygenated phenylindan isomers and their stability in aqueous solution. J. Agric. Food Chem. 44, 898–905.

Švorc, L., Tomčík, P., Svítková, J., Rievaj, M., Bustin, D., 2012. Voltammetric determination of caffeine in beverage samples on bare boron-doped diamond electrode. Food Chem. 135, 1198–1204.

Tahir, M.B., Sagir, M., Shahzad, K., 2019. Removal of acetylsalicylate and methyl-theobromine from aqueous environment using nano-photocatalyst WO_3-TiO_2 @g-C_3N_4 composite. J. Hazard Mater. 363, 205–213.

Telo, J.P., Vieira, A.J.S.C., 1997. Mechanism of free radical oxidation of caffeine in aqueous solution. J. Chem. Soc., Perkin Trans. 2 9, 1755–1758.

Uddin, M.T., Nicolas, Y., Olivier, C., Jaegermann, W., Rockstroh, N., Junge, H., Toupance, T., 2017. Band alignment investigations of heterostructure NiO/TiO_2 nanomaterials used as efficient heterojunction earth-abundant metal oxide photocatalysts for hydrogen production. Phys. Chem. Chem. Phys. 19, 19279–19288.

Vignesh, K., Rhatigan, S., Mathew, S., Michel, M.C., Bartlett, J., Nolan, M., Hinder, S.J., Gascó, A., Ruiz-Palomar, C., Hermosilla, D., 2020. Mo doped TiO_2: impact on oxygen vacancies, anatase phase stability and photocatalytic activity. J. Phys. Math. 3, 025008-025024.

Zeng, Y., Wang, T., Zhang, S., Wang, Y., Zhong, Q., 2017. Sol–gel synthesis of CuO-TiO_2 catalyst with high dispersion CuO species for selective catalytic oxidation of NO. Appl. Surf. Sci. 411, 227–234.

Zhang, F., Li, Y.H., Li, J.Y., Tang, Z.R., Xu, Y.J., 2019. 3D graphene-based gel photocatalysts for environmental pollutants degradation. Environ. Pollut. 253, 365–376.

Zhao, L., Jinghui, D., Sun, P., Liu, J., Ji, Y., Nakada, N., Qiao, Z., Tanaka, H., Yang, Y., 2018. Nanomaterials for treating emerging contaminants in water by adsorption and photocatalysis: systematic review and bibliometric analysis. Sci. Total Environ. 627, 1253–1263.